

# Electrical and Optical Properties of $\alpha$ -(BETS) $_2$ I $_3$ and $\alpha$ -(BEDT-STF) $_2$ I $_3$

Makoto Inokuchi, Hiroyuki Tajima,\* Akiko Kobayashi, Toshiaki Ohta,  
Haruo Kuroda,# Reizo Kato,† Toshio Naito,†† and Hayao Kobayashi††

Department of Chemistry, School of Science, The University of Tokyo, Hongo, Bunkyo-ku, Tokyo 113

†Institute for Solid State Physics, The University of Tokyo, Roppongi, Minato-ku, Tokyo 106

††Department of Chemistry, Faculty of Science, Toho University, Funabashi, Chiba 274

(Received September 6, 1994)

The electrical and optical properties were studied concerning  $\alpha$ -(BETS) $_2$ I $_3$  and  $\alpha$ -(BEDT-STF) $_2$ I $_3$ , which are isostructural to  $\alpha$ -(BEDT-TTF) $_2$ I $_3$ . It has been shown that  $\alpha$ -(BETS) $_2$ I $_3$  and  $\alpha$ -(BEDT-STF) $_2$ I $_3$  undergo metal-insulator transitions at around 50 and 80 K, respectively, and that their electrical resistivities exhibit temperature dependences resembling that of  $\alpha$ -(BEDT-TTF) $_2$ I $_3$  under high pressure. The optical reflectance spectra of these salts show a two-dimensional nature of their electronic structures, and analyses of the spectral data show that the transverse inter-molecular interaction increases in the order  $\alpha$ -(BEDT-TTF) $_2$ I $_3$  <  $\alpha$ -(BEDT-STF) $_2$ I $_3$  <  $\alpha$ -(BETS) $_2$ I $_3$ .

BEDT-TSF (BETS) and BEDT-STF are analogues of BEDT-TTF, different in the respect that some of the S atoms in the TTF skeleton are replaced with Se atoms (see Fig. 1). Both BETS and BEDT-STF form charge-transfer salts with a variety of inorganic anions, as in the case of BEDT-TTF. The crystal structures of these salts have been classified into five categories:  $\kappa$ -type,  $\theta$ -type,  $\lambda$ -type,  $\alpha$ -type, and the others.<sup>1–3)</sup> The  $\kappa$ -,  $\theta$ -, and  $\alpha$ -type crystal structures are analogous to those found in the family of BEDT-TTF salts. All of the  $\kappa$ -type salts of BETS are metallic down to 4.2 K, and the  $\theta$ -type salts are mostly metallic down to 4.2 K although some of them exhibit metal-insulator transitions at low temperatures. The  $\lambda$ -type structure is

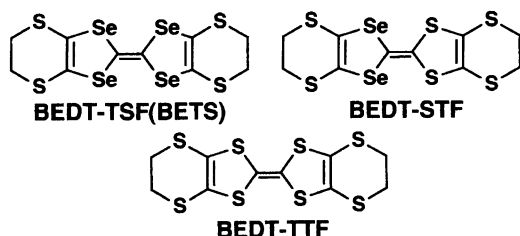


Fig. 1. Molecular structure of BETS (BEDT-TSF), BEDT-STF, and BEDT-TTF. BETS=(BEDT-TSF)=Bis(ethylenedithio)tetraselenafulvalene. BEDT-STF=Bis(ethylenedithio)diselenadithiafulvalene. BEDT-TTF=Bis(ethylenedithio)tetrathiafulvalene.

the one that has been newly found in the following two BETS salts:  $\lambda$ -(BETS) $_2$ GaCl $_4$  and  $\lambda$ -(BETS) $_2$ FeCl $_4$ . The former undergoes a superconducting transition at 8 K,<sup>2)</sup> while the latter undergoes a sharp metal-insulator transition at 8 K.<sup>3)</sup> Since the inter-molecular Se...Se and Se...S contacts in the transverse direction would give a stronger inter-chain interaction compared with the S...S contact, the two-dimensional character is expected to be enhanced in charge-transfer salts involving BETS or BEDT-STF, as compared with the corresponding salts of BEDT-TTF. Thus, BETS and BEDT-STF salts are expected to exhibit some electrical behavior reflecting the increase in the inter-chain interaction. In this respect, it is of great interest to compare the electrical properties of the salts involving BETS and BEDT-STF with those of the corresponding BEDT-TTF salts in order to elucidate the effect of the enhancement of the inter-chain interaction.

In this report we describe studies concerning the electrical resistivity and reflectance spectra on  $\alpha$ -(BETS) $_2$ I $_3$  and  $\alpha$ -(BEDT-STF) $_2$ I $_3$ . The temperature dependence of the resistivity observed for these salts is compared with the behavior of the isostructural salt,  $\alpha$ -(BEDT-TTF) $_2$ I $_3$ . A discussion is also given concerning the transfer integrals derived from analyses of the reflectance spectra of the above-mentioned three salts.

## Experimental

Single crystals of  $\alpha$ -(BETS) $_2$ I $_3$  and  $\alpha$ -(BEDT-STF) $_2$ I $_3$  were electrochemically prepared from 1,1,2-trichloroethane and chlorobenzene solutions, respectively, by using  $n$ -Bu $_4$ Ni $_3$

#Present address: The Research Institutes for Science and Technology, the Science University of Tokyo, 2641 Yamazaki, Noda 278.

Table 1. Crystal Parameters of  $\alpha$ -X $_2$ I $_3$ 

| X=                     |            | $a$   | $b$    | $c$    | $\alpha$ | $\beta$ | $\gamma$ | $V$            |
|------------------------|------------|-------|--------|--------|----------|---------|----------|----------------|
|                        |            | Å     | Å      | Å      | °        | °       | °        | Å <sup>3</sup> |
| BETS                   | $P\bar{1}$ | 9.209 | 10.816 | 17.777 | 96.63    | 97.89   | 90.69    | 1741.5         |
| BEDT-STF               | $P\bar{1}$ | 9.198 | 10.802 | 17.607 | 96.86    | 97.88   | 90.75    | 1719.7         |
| BEDT-TTF <sup>a)</sup> | $P\bar{1}$ | 9.211 | 10.850 | 17.488 | 96.95    | 97.97   | 90.75    | 1717.5         |

a) Ref. 5.

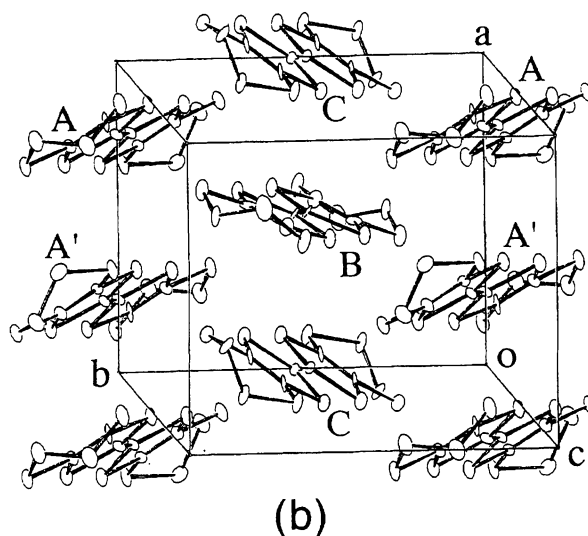
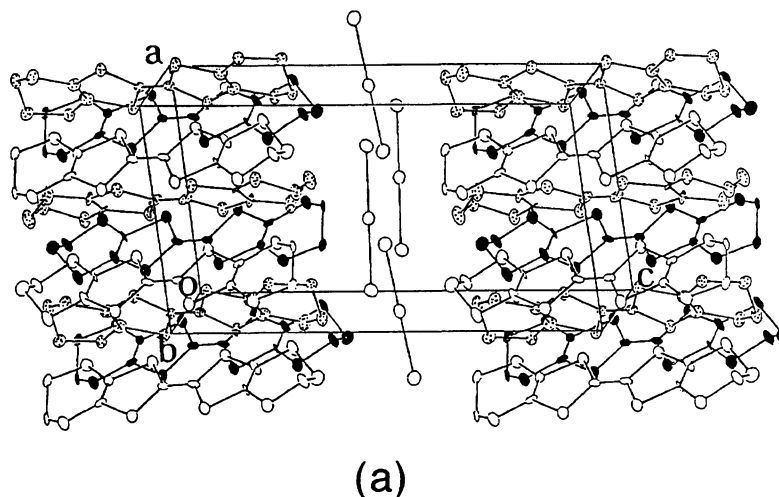


Fig. 2. Crystal structure of  $\alpha$ -(BETS) $_2$ I $_3$ : (a) projection showing conducting and insulating layers, and (b) projection showing the arrangement of BETS $^{1/2+}$  within a conducting layer.

as the supporting electrolyte. Both crystals were obtained as platelets having developed crystal faces of (0 0 1). The electrical resistivity within the (0 0 1) plane was measured by the four-probe method with a d.c. current of 10  $\mu$ A. Four electrical leads of 20  $\mu$ m gold wires were put onto the sample with carbon paste. The polarized reflectance spectra were measured using two kinds of microspectrophotometers on the (0 0 1) crystal face over the wavenumber region from 450 to 25000  $\text{cm}^{-1}$  for the two polarization directions which gave the minimum and maximum reflectivities at 3330  $\text{cm}^{-1}$ . By means of the X-ray diffraction technique, the thus-cho-

sen polarization directions were found to be parallel to the  $a$ - and  $b$ -axes, respectively. The details concerning the measurement procedures of the reflectance spectra have been described elsewhere.<sup>4)</sup>

### Results and Discussion

$\alpha$ -(BETS) $_2$ I $_3$ ,  $\alpha$ -(BEDT-STF) $_2$ I $_3$ , and  $\alpha$ -(BEDT-TTF) $_2$ I $_3$ <sup>5)</sup> are isostructural to each other, having the crystal parameters listed in Table 1. The characteristic features of the  $\alpha$ -type structure are as follows: (1) the

donor molecules with a formal charge of +0.5 form a two-dimensional network in a conducting layer without forming a dimer; (2) four donor molecules are contained in the two-dimensional unit cell within a conducting layer; and (3) each conducting layer is sandwiched by insulating layers of inorganic anions. Figure 2a shows the crystal structure of  $\alpha$ -(BETS)<sub>2</sub>I<sub>3</sub>. The conducting layer of BETS and the insulating layer of I<sub>3</sub><sup>-</sup> are alternately arranged along the *c*\*-axis. Figure 2b shows the molecular arrangement within a conducting layer. There are three crystallographically independent BETS molecules. One, denoted (A), is located on the general position; the other two, denoted (B) and (C), are on the inversion center. In the case of  $\alpha$ -(BEDT-STF)<sub>2</sub>I<sub>3</sub>, the arrangement of BEDT-STF molecules is almost the same as that in  $\alpha$ -(BETS)<sub>2</sub>I<sub>3</sub>, though there exists a partial disorder regarding the orientation of the BEDT-STF molecule because of its asymmetrical molecular geometry.

Figure 3 shows the temperature dependence of the resistivity observed on  $\alpha$ -(BETS)<sub>2</sub>I<sub>3</sub> and  $\alpha$ -(BEDT-STF)<sub>2</sub>I<sub>3</sub> together with the corresponding data of  $\alpha$ -(BEDT-TTF)<sub>2</sub>I<sub>3</sub>. Both  $\alpha$ -(BETS)<sub>2</sub>I<sub>3</sub> and  $\alpha$ -(BEDT-STF)<sub>2</sub>I<sub>3</sub> are metallic at around room temperature; the room-temperature resistivity within the *ab*-plane  $\rho$ (R.T.) is  $6 \times 10^{-3}$ – $4 \times 10^{-2} \Omega \text{ cm}$  in  $\alpha$ -(BETS)<sub>2</sub>I<sub>3</sub> and about  $4 \times 10^{-2} \Omega \text{ cm}$  in  $\alpha$ -(BEDT-STF)<sub>2</sub>I<sub>3</sub>. As can be seen from Fig. 3,  $\alpha$ -(BETS)<sub>2</sub>I<sub>3</sub> undergoes a metal-insulator transition in the temperature range around 50 K and  $\alpha$ -(BEDT-STF)<sub>2</sub>I<sub>3</sub> around 80 K. These transition temperatures are much lower than that of  $\alpha$ -(BEDT-TTF)<sub>2</sub>I<sub>3</sub> (135 K<sup>5)</sup>). The transition from the metallic phase to the insulating phase is not sharp in both  $\alpha$ -(BETS)<sub>2</sub>I<sub>3</sub> and  $\alpha$ -(BEDT-STF)<sub>2</sub>I<sub>3</sub>, showing a gradual increase in the resistivity upon lowering the temperature over a considerably wide temperature range, whereas the transition is relatively sharp in  $\alpha$ -(BEDT-TTF)<sub>2</sub>I<sub>3</sub>. It should also be noted that, in the case of  $\alpha$ -(BETS)<sub>2</sub>I<sub>3</sub>, there is an indication for the existence of another kind of phase transition at around 40 K. The above-described features in the temperature dependence of the resistivity observed on  $\alpha$ -(BETS)<sub>2</sub>I<sub>3</sub> and  $\alpha$ -(BEDT-STF)<sub>2</sub>I<sub>3</sub> are more or less similar to those observed on  $\alpha$ -(BEDT-TTF)<sub>2</sub>I<sub>3</sub> under high pressure.<sup>6)</sup>

In Fig. 4, the temperature dependence of the resistivities is plotted as  $\log [\rho(T)/\rho(\text{R.T.})]$  versus  $1/T$ . Both in  $\alpha$ -(BETS)<sub>2</sub>I<sub>3</sub> and in  $\alpha$ -(BEDT-STF)<sub>2</sub>I<sub>3</sub>, the  $\rho(T)$  data in the insulating phase can not be fitted with a single exponential function of the type  $\rho(T) \propto \exp(E_a/k_B T)$ . If we apply the above equation to the data only within a narrow temperature range below the metal-insulator transition, the activation energy ( $E_a$ ) is estimated to be 0.019 eV ( $T \approx 45$  K) for  $\alpha$ -(BETS)<sub>2</sub>I<sub>3</sub> and 0.029 eV ( $T \approx 55$  K) for  $\alpha$ -(BEDT-STF)<sub>2</sub>I<sub>3</sub>, the corresponding value being as large as 0.14 eV ( $T \approx 120$  K) for  $\alpha$ -(BEDT-TTF)<sub>2</sub>I<sub>3</sub>. The above results could mean that the energy gap ( $2E_a$ ) in the insulating phase is roughly

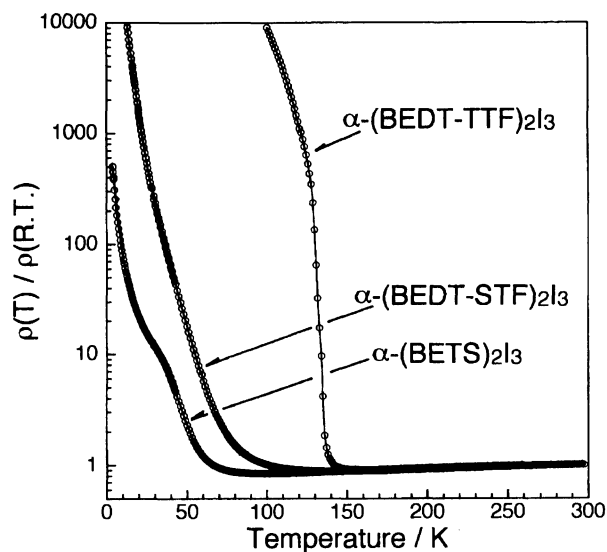


Fig. 3. Temperature dependence of the electrical resistivity of  $\alpha$ -(BETS)<sub>2</sub>I<sub>3</sub>,  $\alpha$ -(BEDT-STF)<sub>2</sub>I<sub>3</sub>, and  $\alpha$ -(BEDT-TTF)<sub>2</sub>I<sub>3</sub> within the *ab*-plane: The logarithm of resistivity is plotted versus the temperature.

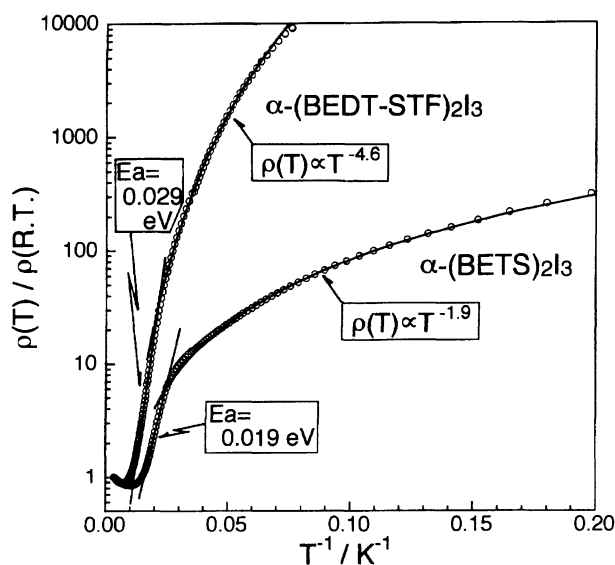


Fig. 4. Plot of the logarithm of the resistivity versus reciprocal temperature for  $\alpha$ -(BETS)<sub>2</sub>I<sub>3</sub> and  $\alpha$ -(BEDT-STF)<sub>2</sub>I<sub>3</sub>.

0.04 eV for  $\alpha$ -(BETS)<sub>2</sub>I<sub>3</sub> and 0.06 eV for  $\alpha$ -(BEDT-STF)<sub>2</sub>I<sub>3</sub>, and that a much wider band gap opens in  $\alpha$ -(BEDT-TTF)<sub>2</sub>I<sub>3</sub> upon going from the metallic phase to the insulating phase. The temperature dependence of the resistivity in the lower temperature region can be well fitted with the equation  $\rho(T) \propto T^{-\alpha}$ . The value of  $\alpha$  was found to be 1.9 for  $\alpha$ -(BETS)<sub>2</sub>I<sub>3</sub> ( $T < 20$  K) and 4.6 for  $\alpha$ -(BEDT-STF)<sub>2</sub>I<sub>3</sub> ( $T < 35$  K).

Figures 5a and 5b show the reflectance spectra of  $\alpha$ -(BETS)<sub>2</sub>I<sub>3</sub> and  $\alpha$ -(BEDT-STF)<sub>2</sub>I<sub>3</sub> observed at room temperature on the (0 0 1) crystal face for the light polarizations parallel to the *a*-axis ( $E//a$ ) and to the *b*-axis ( $E//b$ ). As can be seen from these figures, the spec-

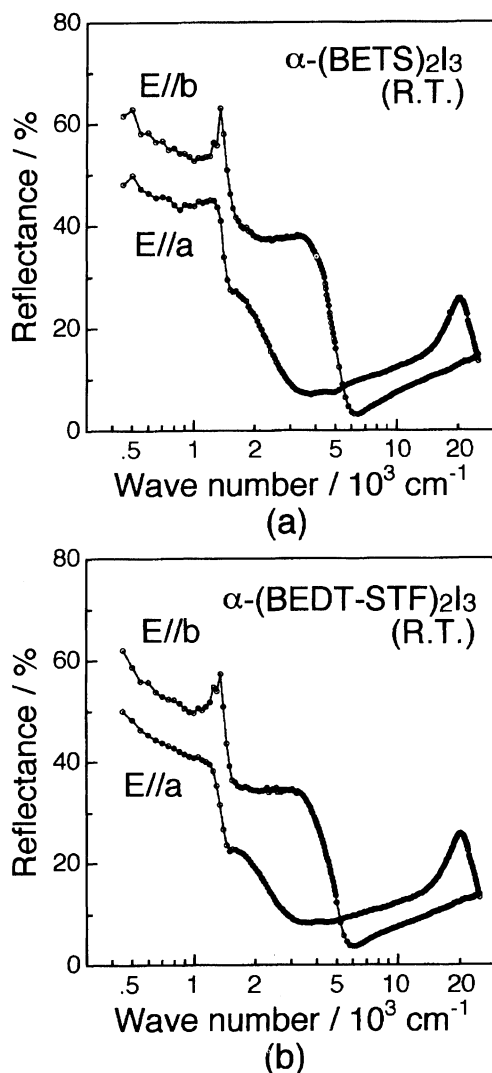


Fig. 5. Reflectance spectra of (a)  $\alpha$ -(BETS)<sub>2</sub>I<sub>3</sub> and (b)  $\alpha$ -(BEDT-STF)<sub>2</sub>I<sub>3</sub> at room temperature.

tra of the two salts are almost identical to each other, showing the following common features. A metallic dispersion appears in both the  $E//a$  spectrum and the  $E//b$  spectrum with an almost comparable intensity between the two spectra. This fact indicates the two-dimensional nature of the electronic structures. The broad dispersion at around 20000  $\text{cm}^{-1}$  in the  $E//a$  spectrum is attributable to the electronic transition within the  $\text{I}_3^-$  ion, elongating roughly along the  $a$ -axis; also, a sharp peak in the infrared region at about 1300  $\text{cm}^{-1}$  in both the  $E//b$  and  $E//a$  spectra can be attributed to the vibrational transition of  $[\text{BETS}]^{1/2+}$  (or  $[\text{BEDT-STF}]^{1/2+}$ ) coupled with the charge-transfer excitation.

Figure 6 shows the temperature dependence of the reflectance spectra of  $\alpha$ -(BETS)<sub>2</sub>I<sub>3</sub>. The temperature dependence of  $\alpha$ -(BEDT-STF)<sub>2</sub>I<sub>3</sub> was found to be essentially the same as that of  $\alpha$ -(BETS)<sub>2</sub>I<sub>3</sub>. We thus do not show here the spectral data of  $\alpha$ -(BEDT-STF)<sub>2</sub>I<sub>3</sub>. The following description can be applied to  $\alpha$ -(BEDT-STF)<sub>2</sub>I<sub>3</sub>, although we concentrate our discussion only

on  $\alpha$ -(BETS)<sub>2</sub>I<sub>3</sub>. As expected, the dispersion due to the  $\text{I}_3^-$  anion, which appears at around 20000  $\text{cm}^{-1}$  in the  $E//a$  spectrum, becomes sharper upon lowering the temperature. The metallic dispersion in the infrared region is rather weakly dependent on the temperature, and no abrupt change appears upon the metal-insulator transition. This is markedly different from what has been observed on  $\alpha$ -(BEDT-TTF)<sub>2</sub>I<sub>3</sub>: A concavity does appear at 2600  $\text{cm}^{-1}$  and the reflectivity in the wavenumber region below 1000  $\text{cm}^{-1}$  significantly decreases below the transition temperature.<sup>4)</sup> Seemingly, little change in the reflectance spectra and the lack of a steep increase in the electrical resistivity on the metal-insulator transition of  $\alpha$ -(BETS)<sub>2</sub>I<sub>3</sub> ( $\alpha$ -(BEDT-STF)<sub>2</sub>I<sub>3</sub>) suggest that the transition is either a second-order transition or a first-order transition with a small change of the order parameter; the transition in  $\alpha$ -(BEDT-TTF)<sub>2</sub>I<sub>3</sub> was found to be first-order by a specific-heat measurement,<sup>7)</sup> although the nature of the transition has not yet been clarified.

Figure 7 shows the optical-conductivity spectra over the region up to 12000  $\text{cm}^{-1}$ , which have been calculated through a Kramers-Krönig transformation of the reflectance spectra shown in Fig. 6. The  $E//a$  conductivity spectra show a vibrational peak at about 1000  $\text{cm}^{-1}$  superimposed over a Drude-like absorption. In the  $E//b$  conductivity spectra, a broad absorption band centered at about 3000  $\text{cm}^{-1}$  and a sharp vibrational peak at 1250  $\text{cm}^{-1}$  are superimposed over a Drude-like absorption. The broad absorption band in the  $E//b$  spectra can be ascribed to an inter-band transition between the two bands formed from HOMO's of donor molecules, as is often observed on BEDT-TTF salts.<sup>8)</sup> In the insulating phase of  $\alpha$ -(BEDT-TTF)<sub>2</sub>I<sub>3</sub>, the conductivity spectrum is known to exhibit an indication for the opening of an optical gap. Such an indication for the existence of an optical gap can be found neither in the conductivity spectra of  $\alpha$ -(BETS)<sub>2</sub>I<sub>3</sub> at 25 K, nor in the spectra of the insulating phase of  $\alpha$ -(BEDT-STF)<sub>2</sub>I<sub>3</sub>. This fact suggests that the band gap in the insulating phase, if it exists, should be less than 0.08 eV (=650  $\text{cm}^{-1}$ ) for  $\alpha$ -(BETS)<sub>2</sub>I<sub>3</sub> and  $\alpha$ -(BEDT-STF)<sub>2</sub>I<sub>3</sub>. As we have already mentioned, the activation energy estimated from the temperature dependence of the resistivity in the narrow temperature range below the transition temperature was found to be 0.019, 0.029 and 0.14 eV in  $\alpha$ -(BETS)<sub>2</sub>I<sub>3</sub>,  $\alpha$ -(BEDT-STF)<sub>2</sub>I<sub>3</sub>, and  $\alpha$ -(BEDT-TTF)<sub>2</sub>I<sub>3</sub>, respectively. Seemingly, this is consistent with the conclusion derived from the optical conductivity spectra.

From the Drude-like component in the observed optical conductivity spectra, we estimated the plasma frequency ( $\omega_p$ ) using the following equation:

$$\omega_p^2 = 8 \int \sigma(\omega) d\omega. \quad (1)$$

The integration was performed over the 0–8000  $\text{cm}^{-1}$

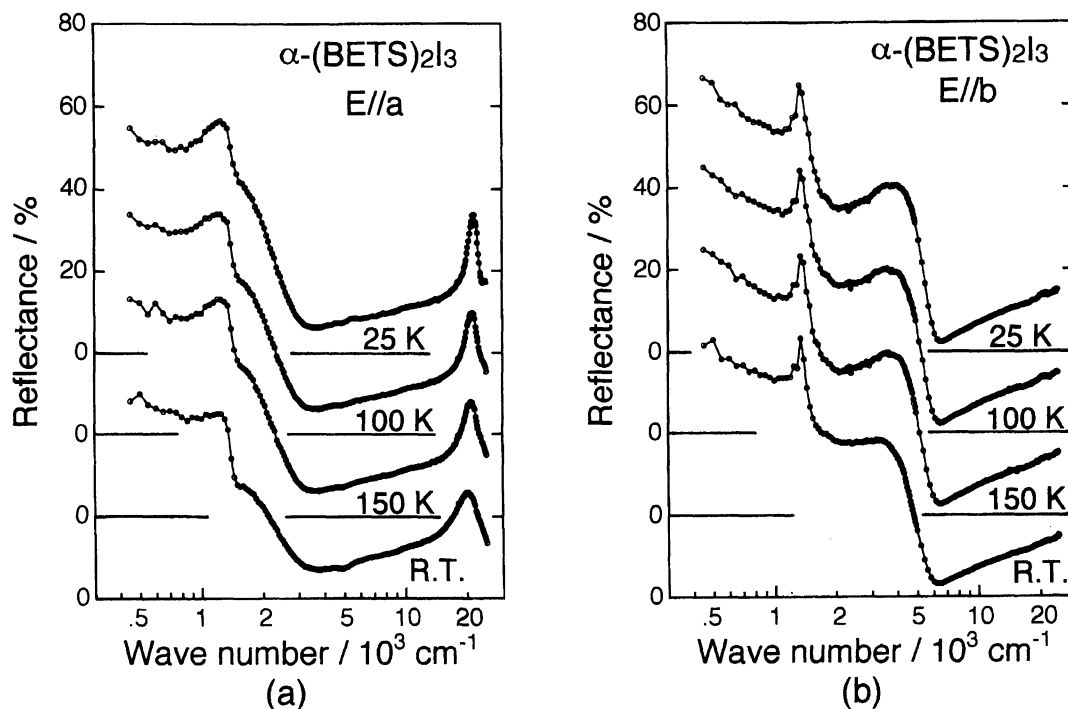


Fig. 6. Temperature dependence of the reflectance spectra of  $\alpha$ -(BETS) $_2$ I $_3$ : (a) the  $E//a$  spectra and (b) the  $E//b$  spectra.

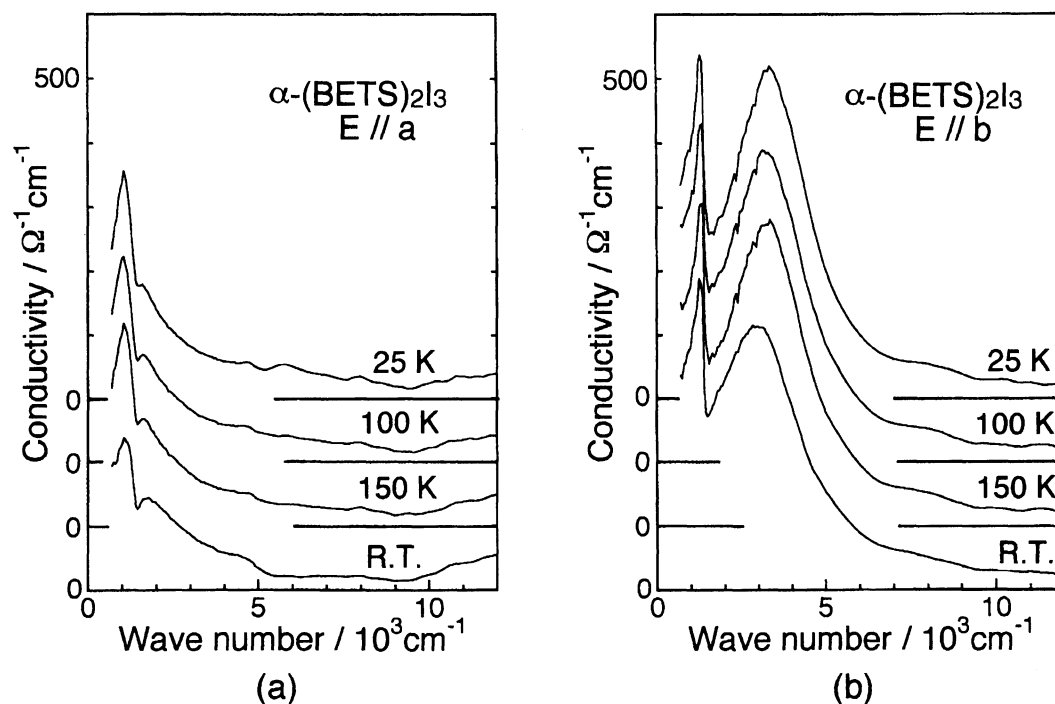


Fig. 7. Temperature dependence of the optical-conductivity spectra of  $\alpha$ -(BETS) $_2$ I $_3$  obtained through a Kramers–Krönig transformation of Fig. 6: (a) the  $E//a$  spectra and (b) the  $E//b$  spectra.

wavenumber region. In order to estimate the transfer integrals from the thus-determined plasma frequencies, we adopted a simplified model (shown in Fig. 8b) based on the  $\theta$ -type structure.<sup>9)</sup> The  $\theta$ -type structure can be regarded as being a special case of the  $\alpha$ -type struc-

ture having two crystallographically equivalent donor molecules in the two-dimensional unit cell of the conducting layer. The effective transfer integrals ( $t_1$  and  $t_2$ ) defined in Fig. 8b should be regarded as being weighted averages of several different transfer integrals in an ac-

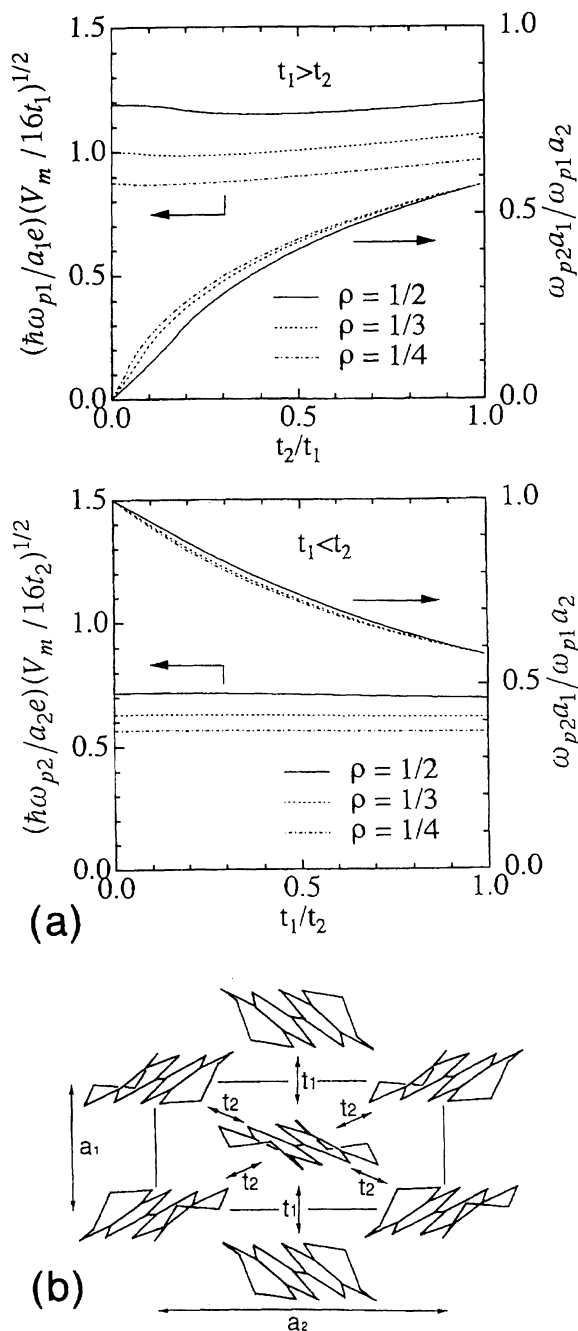


Fig. 8. (a) Relation between the plasma frequencies ( $\omega_{p1}$ ,  $\omega_{p2}$ ) and the transfer integrals ( $t_1$ ,  $t_2$ ) based on the two-dimensional tight-binding model having a  $\theta$ -type structure. The calculation was carried out for the three cases of  $\rho=1/2$ ,  $1/3$ , and  $1/4$ , where  $\rho$  denotes the degree of charge transfer of a donor molecule forming a conducting layer. The Fermi surface is open in the range of  $t_2/t_1 < 0.18$ ,  $0.08$  and  $0.04$  for  $\rho=1/2$ ,  $1/3$  and  $1/4$ , respectively. (b) The definition of the effective transfer integrals ( $t_1$ ,  $t_2$ ), and the lattice spacing ( $a_1$ ,  $a_2$ ).

tual  $\alpha$ -type structure. When we adopt the above simplified model, the energy dispersion ( $\varepsilon(\vec{k})$ ) of the two-dimensional band structure can be expressed as

Table 2. The Plasma Frequencies and Mean Transfer Integrals of  $\alpha$ -(BETS) $_2$ I $_3$ ,  $\alpha$ -(BEDT-STF) $_2$ I $_3$ , and  $\alpha$ -(BEDT-TTF) $_2$ I $_3$  at Room Temperature

|                                  | $\omega_{p1}$<br>eV | $\omega_{p2}$<br>eV | $t_1$<br>eV | $t_2$<br>eV |
|----------------------------------|---------------------|---------------------|-------------|-------------|
| $\alpha$ -(BETS) $_2$ I $_3$     | 0.60                | 1.05                | 0.036       | 0.071       |
| $\alpha$ -(BEDT-STF) $_2$ I $_3$ | 0.59                | 0.99                | 0.036       | 0.063       |
| $\alpha$ -(BEDT-TTF) $_2$ I $_3$ | 0.55                | 0.82                | 0.035       | 0.043       |

$$\varepsilon(\vec{k}) \equiv \varepsilon(k_1, k_2)$$

$$= 2t_1 \cos(a_1 k_1) \pm 4t_2 \cos(a_1 k_1/2) \times \cos(a_2 k_2/2), \quad (2)$$

where  $t_i$  ( $i=1, 2$ ) and  $a_i$  ( $i=1, 2$ ) are the effective transfer integrals and the lattice spacings, respectively. The plasma frequencies can be calculated by the following Lindhard equation:<sup>10)</sup>

$$\omega_{pi}^2 = \frac{4\pi n e^2}{(m_{opt})_i},$$

$$\frac{1}{(m_{opt})_i} \equiv \frac{\int f(\varepsilon(\vec{k})) \frac{\partial^2 \varepsilon}{\partial k_i^2} dk}{\int f(\varepsilon(\vec{k})) dk}, \quad (3)$$

where  $f(\varepsilon)$  denotes the Fermi-Dirac distribution function. By using Eqs. 2 and 3, a numerical calculation of the relation between ( $\omega_{p1}$ ,  $\omega_{p2}$ ) and ( $t_1$ ,  $t_2$ ) was performed; the results are shown in Fig. 8a.

Using Fig. 8a ( $\rho=1/2$ ), the effective transfer integrals ( $t_1$ ,  $t_2$ ) of  $\alpha$ -(BETS) $_2$ I $_3$ ,  $\alpha$ -(BEDT-STF) $_2$ I $_3$ , and  $\alpha$ -(BEDT-TTF) $_2$ I $_3$  at room temperature were estimated. The plasma frequencies ( $\omega_{p1}$ ,  $\omega_{p2}$ ) were determined from the room-temperature optical conductivity spectra, and the values of  $a_1=a/2$ ,  $a_2=b$  and  $V_m=V/2$  ( $V$  is the unit cell volume) were derived from the crystal data given in Table 1. The obtained results are listed in Table 2. It should be noted that both  $\omega_{p1}$  and  $\omega_{p2}$  increase in the order  $\alpha$ -(BEDT-TTF) $_2$ I $_3$  <  $\alpha$ -(BEDT-STF) $_2$ I $_3$  <  $\alpha$ -(BETS) $_2$ I $_3$ , and that the transfer integral ( $t_2$ ), which is mainly associated with the transverse inter-molecular interaction, also increases in the same order; the other transfer integral ( $t_1$ ) remains almost the same for the three salts. If we compare the above result with the difference among the electrical behavior of the three salts (shown in Fig. 3) we can see that there is some correlation between the change in the electrical behavior and the increase of the transverse inter-molecular interaction. As we have mentioned earlier, the temperature dependence of the electrical resistivity observed on  $\alpha$ -(BETS) $_2$ I $_3$  or  $\alpha$ -(BEDT-STF) $_2$ I $_3$  is more or less like that observed on  $\alpha$ -(BEDT-TTF) $_2$ I $_3$  under high pressures. It is also known that the metal-insulator transition is suppressed by applying 4.5 kbar in  $\alpha$ -(BETS) $_2$ I $_3$ ,<sup>11)</sup> while 12 kbar should be applied in  $\alpha$ -(BEDT-TTF) $_2$ I $_3$ .<sup>6)</sup> All of these facts suggest that  $\alpha$ -(BETS) $_2$ I $_3$  and  $\alpha$ -(BEDT-STF) $_2$ I $_3$  can be regarded as being in the states corresponding to a pressurized state

of  $\alpha$ -(BEDT-TTF)<sub>2</sub>I<sub>3</sub>. This is possibly associated with an increase in the transverse inter-molecular interaction through Se...Se and/or Se...S contacts.

### Summary and Conclusion

We have investigated the electrical and optical properties of  $\alpha$ -(BETS)<sub>2</sub>I<sub>3</sub> and  $\alpha$ -(BEDT-STF)<sub>2</sub>I<sub>3</sub> and compared them with those of the isostructural BEDT-TTF salt,  $\alpha$ -(BEDT-TTF)<sub>2</sub>I<sub>3</sub>. From analyses of the optical reflectance spectra, we found that the transfer integral related to the transverse inter-molecular interaction increases in the order  $\alpha$ -(BEDT-TTF)<sub>2</sub>I<sub>3</sub> <  $\alpha$ -(BEDT-STF)<sub>2</sub>I<sub>3</sub> <  $\alpha$ -(BETS)<sub>2</sub>I<sub>3</sub>, as can be expected from the effect due to an increased interaction through inter-molecular Se...Se contacts. The electrical behavior, such as the temperature dependence of the electrical resistivity, varies following the same order  $\alpha$ -(BEDT-TTF)<sub>2</sub>I<sub>3</sub> →  $\alpha$ -(BEDT-STF)<sub>2</sub>I<sub>3</sub> →  $\alpha$ -(BETS)<sub>2</sub>I<sub>3</sub>. Seemingly, these facts suggest that the difference in the electrical behavior found among the three salts reflects an increase in the transverse inter-molecular interaction. However, a further investigation will be needed in order to understand the nature of the metal-insulator transition in the three salts.

We wish to acknowledge Professor Kyuya Yakushi for providing us with the reflectance spectra data of  $\alpha$ -(BEDT-TTF)<sub>2</sub>I<sub>3</sub>. We thank Mr. Masafumi Tamura for his help in measuring of the reflectance spectra. This work was partly supported by a Grant-in-Aid for the Special Project Research on the "Molecular conductors" No. 06243208 from the Ministry of Education, Science and Culture.

### References

- 1) a) R. Kato, H. Kobayashi, and A. Kobayashi, *Synth. Met.*, **41—43**, 2093 (1991); b) T. Naito, A. Miyamoto, H. Kobayashi, R. Kato, and A. Kobayashi, *Chem. Lett.*, **1991**, 1945; c) L. K. Montgomery, T. Burgin, C. Husting, L. Tilley, J. C. Huffmann, K. D. Carlson, J. D. Dudek, G. A. Yaconi, U. Geiser, and J. M. Williams, *Mol. Cryst. Liq. Cryst.*, **211**, 283 (1992); d) A. Kobayashi, R. Kato, T. Naito, and H. Kobayashi, *Synth. Met.*, **56**, 2078 (1993).
- 2) H. Kobayashi, T. Udagawa, H. Tomita, K. Bun, T. Naito, and A. Kobayashi, *Chem. Lett.*, **1993**, 1559.
- 3) A. Kobayashi, T. Udagawa, H. Tomita, T. Naito, and H. Kobayashi, *Chem. Lett.*, **1993**, 2179.
- 4) K. Yakushi, H. Kanbara, H. Tajima, H. Kuroda, G. Saito, and T. Mori, *Bull. Chem. Soc. Jpn.*, **60**, 4251 (1987).
- 5) K. Bender, I. Henning, D. Schweitzer, K. Dietz, H. Endres, and H.J. Keller, *Mol. Cryst. Liq. Cryst.*, **108**, 359 (1984).
- 6) a) H. Schwenk, F. Gross, C-P. Heidmann, K. Andres, D. Schweitzer, and H. Keller, *Mol. Cryst. Liq. Cryst.*, **119**, 329 (1985); b) M. V. Kartsovnik, P. A. Kononovich, V. N. Laukhin, A. G. Khomenko, and I. F. Shchegolev, *Sov. Phys. JETP*, **61**, 866 (1985); c) K. Kajita, T. Ojio, H. Fujii, Y. Nishio, H. Kobayashi, A. Kobayashi, and R. Kato, *J. Phys. Soc. Jpn.*, **61**, 23 (1992).
- 7) N. A. Fortune, K. Murata, M. Ishibashi, M. Tokumoto, N. Kinoshita, and H. Anzai, *Solid State Commun.*, **77**, 265 (1991).
- 8) H. Kuroda, K. Yakushi, H. Tajima, A. Ugawa, M. Tamura, Y. Okawa, A. Kobayashi, R. Kato, H. Kobayashi, and G. Saito, *Synth. Met.*, **27**, A491 (1988).
- 9) a) H. Kobayashi, R. Kato, A. Kobayashi, Y. Nishio, K. Kajita, and W. Sasaki, *Chem. Lett.*, **1986**, 833; b) M. Tamura, K. Yakushi, H. Kuroda, A. Kobayashi, R. Kato, and H. Kobayashi, *J. Phys. Soc. Jpn.*, **57**, 3239 (1988).
- 10) For example : F. Wooten, "Optical Properties of Solid," Academic Press, New York (1972).
- 11) M. Inokuchi, H. Tajima, A. Kobayashi, H. Kuroda, R. Kato, T. Naito, and H. Kobayashi, *Synth. Met.*, **56**, 2495 (1993).